UNCLASSIFIED
(Approved for Publication)

CLM - P 13

On the Origin of B_θ, $v_{poloidal}$ and v_θ in the Conical θ Pinch

by

W. H. BOSTICK*
Stevens Institute of Technology

D. R. WELLS
Plasma Physics Laboratory, Princeton

A B S T R A C T

A simple current-sheet model of a hydromagnetic shock is employed in an attempt to explain the origin of the B_θ and $v_{poloidal}$ observed in the hydromagnetic vortex rings[1,2] produced in the conical θ pinch. Although this simple model has its limitations, it nevertheless shows clearly that the B_θ and the vortex structure are due to Hall currents which are driven by shear in acceleration, and that the existence of any right-handedness and left-handedness and of the plasma vortex structure itself depends upon the fact that negative electricity (electrons) are light and positive electricity (protons) are heavy. The model also gives a plausible explanation and description of the origin of θ rotation, i.e. v_θ in the θ pinch.

(Submitted for publication in 'Physics of Fluids')

*On NSF Fellowship at Groupe de Recherches de l'association EURATOM CEA, Fontenay-aux-Roses, France & at the Culham Laboratory, England.

U.K.A.E.A. Research Group,
Culham Laboratory,
Nr. Abingdon,
BERKS.

August, 1962
(C.18)

1. This paper treats the process of production of plasma vortex motion and B_θ in the conical θ pinch.

2. The analysis of the coaxial plasma accelerator with a large ratio of outer to inner radius has been made[3] with the model of a simple current sheet. Even this simple model predicts the plasma vortices, perturbation magnetic fields in the θ direction produced by Hall currents, and a different behaviour when the polarity of the center conductor is reversed. The present paper applies this same type of analysis and model for the conical θ pinch and predicts the formation (with the correct sign) of $v_{poloidal}$ and B_θ, both of which have been observed[1,2] in the plasma vortex rings produced in the θ pinch. The $B_{poloidal}$ is, of course, also observed in these vortex rings.

3. Fig.1 shows a conical θ pinch coil with the applied magnetic field B_a and with the dimensions shown. The induced θ electric field E_θ and the induced θ current density $j_{\theta\ ind}$ are also indicated. A first estimate for the thickness δ of the current sheet would be the Rosenbluth sheath thickness, $(\frac{m_e}{2n\mu_o e^2})^{\frac{1}{2}}$ or the Larmor radius of the positive ion. For $n = 10^{14}/cm^3 = 10^{20}/m^3$, the Rosenbluth sheath is about 0.4 mm. For a hydrogen ion of velocity 10^7/cm/sec the Larmor radius is 0.2 mm in a magnetic field of 50,000 gauss and 1 mm in a magnetic field of 10,000 gauss. These values for δ are less than the observed 1 cm thickness for hydrogen reported by Burkhardt and Lovberg[4] and the 5 cm thickness for argon reported by Keck et al[5] for a coaxial accelerator. The processes which go on within the current sheet and which control its thickness are thus obviously more complicated than we might first estimate. For simplicity in exposition we will nevertheless assume a simple current sheet which acts like a shock, even though a substantial amount of current flows behind this current sheet.

4. The co-ordinate ξ is introduced in Fig.1 to represent displacement in the direction perpendicular to the surface of the coil. The co-ordinates η and $r\theta$ are introduced to denote displacements parallel to the surface of the coil. Fig.2 attempts to show the flow through the current sheet (which is essentially a shock front) where, for example, $\dot{\xi}_1$ represents the ξ component of the plasma velocity before entering the shock front and $\dot{\xi}_2$ the ξ component upon leaving the shock front. Even though some current will flow also behind the shock front, it will be assumed for simplicity that a large spacial step in the field B_a occurs in the shock front or current sheet because of the large portion of the total current which flows there.

5. The various portions of the shock front are acted upon by an applied field $B_a(z)$ which depends upon the position z. Therefore the acceleration $\ddot{\xi}$ of the

various portions of plasma in the shock front is different. The electrons carry the major portion of the current $\mathbb{J}_{\theta\ ind}$ and are acted upon by the force $\mathbb{J}_{\theta\ ind} \times \mathbb{B}_a$ which drives them in the ξ direction. The heavier positive ions lag behind, thereby producing the electric field $E_\xi = \frac{m_i}{e}\ddot{\xi}$, which is an active emf and which is prepared to drive currents wherever they are permitted to flow.

6. In the coaxial accelerator the return circuit[3] for the flow of the Hall currents driven by this emf is partially through the metal electrodes. In the conical θ pinch the flow of these Hall currents which are poloidal currents $\mathbb{J}_p$, is through the plasma and is diagrammed in Figs.1 and 2 and produces B_θ as shown. In the coaxial accelerator these particular Hall currents undoubtedly play some part in setting up the shear in velocities which produces rotation in the vortex or eddy. In the conical θ pinch the force, $\mathbb{f}_\theta = \mathbb{J}_p \times \mathbb{B}_a$, which acts primarily upon the electrons, is shown in Figs.1 and 2.

7. In order to understand some of these effects in a semi-quantitative way we start with the equations of conservation of flow of mass, momentum, and energy across the current sheet of thickness δ. An eddy (the observed $v_{poloidal}$)[1,2] will be produced as it is also expected to be produced in the coaxial accelerator when the center conductor is negative. Under these conditions the coaxial accelerator exhibits a planar current sheet. We will therefore assume that the current sheet in the conical θ pinch remains parallel to the coil as it moves inward. In the frame of reference of this current sheet the unshocked plasma approaches the current sheet with a velocity $\dot{\xi}_1$, as shown in Fig.2 and recedes from the current sheet with a velocity which is the vector sum of $\dot{\xi}_2 + \dot{\eta}_2$. The conservation equations for any value of z are thus:-

Mass:
$$n_1 m_i \dot{\xi}_1 = (1 + \frac{\delta}{r_s}) n_2 m_i \dot{\xi}_2 + n_2 m_i \dot{\eta}_2 \cong n_2 m_i \dot{\xi}_2 + n_2 m_i \dot{\eta}_2 \qquad (1)$$

$$\text{if } \frac{\delta}{r_s} \ll 1$$

Momentum:
$$n_1 m_i \dot{\xi}_1^2 - \frac{B_2^2}{2\mu_o} = n_2 m_i \dot{\xi}_2^2 \qquad (2)$$

$$-\delta \frac{d}{d\eta} \left(\frac{B^2}{2\mu_o}\right) - \delta \frac{d}{d\eta}(nkT) = n_2 m_i \dot{\eta}_2 \dot{\xi}_2 \qquad (3)$$

$$\delta(\dot{J}_p \times B_a) = \delta\ \theta = n_2 m_e \dot{\xi}_2 (r\theta)_e = n_2 m_i \dot{\xi}_2 (r\dot{\theta})_{i\ later} \qquad (4)$$

Energy: $\dot{\xi}_1\left[\frac{n_1 m_i \dot{\xi}_1^2}{2} + n_1 kT_1\right] + \dot{\xi}_1 n_1 kT_1 - \frac{B_2^2}{2\mu_o}\dot{\xi}_2 - \dot{\xi}_2 n_2 kT_2$

Rate of Energy Transport into current sheet

Rate of work by pressure terms at the boundaries of the current sheet

$$= \dot{\xi}_2\left[\frac{n_2 m_i \dot{\xi}_2^2}{2} + n_2 kT_2 + \frac{n_2 m_i \dot{\eta}_2^2}{2} + \frac{B_\theta^2}{2\mu_o}\right] \qquad (5)$$

Rate of energy transport away from current sheet.

8. The limitaions of assuming that all the physical facts can be explained in detail by the conditions at the boundaries of the shock or current sheet are evident from these equations. To keep n_2 from becoming infinite at z = o it is necessary to have some $\dot{\eta}$ flow in equation (1). We assume that this $\dot{\eta}$ flow is generated within the sheet and we attempt to account for the momentum change in the η direction with equation (3). Equation (3) is not completely satisfactory because the conversion of flow to the η direction is occurring within the sheet due to the build-up of a grad nkT and to $\frac{d}{d\eta}(\frac{B_a^2}{2\mu_o})$ within the sheet, and we are purposely trying to avoid the exploration of conditions within the sheet. The $\frac{n_2 m_i \dot{\eta}_2^2 \dot{\xi}_2}{2}$ term in equation (5) is not adequately covered by any of the rate-of-work terms in equation (5). Nevertheless, we will proceed with this simple shock model and the equations (1)-(5) because they predict several of the physical effects which are observed.

9. The value of the magnetic field at the exit boundary of the current sheet is:

$$B_2 = (B_o \sin \omega t \frac{\pi r_c^2 - \pi r_s^2}{(\pi r_c^2 - \pi r_s^2)}\Big|_{z=0} = \frac{B_o \sin \omega t\ (\pi r_{co}^2 - \pi r_{so}^2)}{\pi(r_{co} + z \tan \alpha)^2 - \pi(r_{so} + z \tan \alpha)^2}$$

$$= \frac{B_o \sin \omega t}{1 + \frac{2z \tan \alpha}{r_{co} + r_{so}}} = \frac{B_o \sin \omega t}{1 + \frac{2z \tan \alpha}{2r_{co} - \xi/\cos \alpha}}$$

For the initial stages where

$$\xi \ll r_{co},\ B_2 \cong B_o \sin \omega t \left(\frac{1}{1 + \frac{z \tan \alpha}{r_{co}}}\right) = \frac{r_{co}}{r_c} B_o \sin \omega t. \qquad (7)$$

In the later stages where r_s is essentially zero at $z = o_2$ and

$$r_s \ll r_c \text{ at } z = z_m,\ B_2 = \left(\frac{r_{co}}{r_c}\right)^2 B_o \sin \omega t. \qquad (8)$$

10. As an alternative between the varying conditions represented by equations (7) and (8), one might assume, for computational simplicity, that B_2 would fall off linearly with a characteristic length z_m which would be somewhat greater than the length of the coil.

Thus $$B_2 = (1 - \frac{z}{z_m})B_o \sin \omega t = (\frac{r_{cm} - r_c}{r_{cm} - r_{co}})B_o \sin \omega t \qquad (9)$$

For the quantity $(\frac{B_2}{B_o})^2$ at $z = z_m$ (i.e. at $r_c = r_{cm}$) equation (7) gives $\frac{1}{9}$, equation (8) gives $\frac{1}{81}$, and equation (9) gives zero, for

$$\frac{r_{cm}}{r_{co}} = \frac{r_c(z = z_m)}{r_c(z = o)} = 3.$$

Thus it can be assumed that the magnetic pressure step across the current sheet at effective values of $\frac{r_{cm}}{r_{co}} = 3$ is essentially zero. In these circumstances equations (1) and (2) tell us that at $z = z_m$, $\dot{\xi}_2 \cong \dot{\xi}_1$, $n_2 \cong n_1$, and hence $\dot{\eta}_2 \cong 0$. This situation is then analogous to the case of the coaxial accelerator where the radial flow is assumed to be zero at the wall of the outer conductor.

11. In a situation similar to that of the coaxial accelerator[3],

$$\dot{\xi}_1 \eta_1 eE_\xi \frac{\delta}{\frac{\dot{\xi}_1 + \dot{\xi}_2}{2}} = \frac{B_2^2}{2\mu_o},$$

and for the situations where $\dot{\xi}_2 \ll \dot{\xi}_1$

$$eE_\xi \cong \frac{B_2^2}{2\mu_o} \cdot \frac{1}{2n_1\delta}$$

Let us take, for example, the case where $\tan \alpha \cong 0.5$ and $\frac{r_{cm}}{r_{co}} = 3$
Then at $z = z_m$, $\dot{\eta}_2$ is expected to be zero and equation (1) gives

$$n_1 m_i \dot{\xi}_1 = n_2(z_m) m_i \dot{\xi}_2(z_m) \qquad (10)$$

and equation (2) gives

$$n_1 m_i \dot{\xi}_1^2 - \frac{B_o^2 \sin^2 \omega t}{2\mu_o}(\tfrac{1}{2})^2 = n_2(z_m) m_i \dot{\xi}_2^2(z_m) \qquad (11)$$

at $z = o$, $\dot{\xi}_2$ is assumed to be small compared to $\dot{\xi}_1$ and equation (2) gives

$$n_1 m_i \dot{\xi}_1^2 - \frac{B_o^2 \sin^2 \omega t}{2\mu_o} = 0 \qquad (12)$$

Thus

$$n_1 m_i \dot{\xi}_1^2 (1 - \tfrac{1}{9}) = n_2(z_m) m_i \dot{\xi}_2^2(z_m)$$

and

$$\dot{\xi}_2(z_m) \cong \tfrac{8}{9} \dot{\xi}_1, \text{ and } n_2(z_m) \cong \tfrac{9}{8} n_1.$$

12. There must be a large grad $n = \frac{dn}{d\eta}$ within the current sheet in the absence of $\dot{\eta}$ flow. We will assume, however, as we have in the coaxial accelerator[3] that the $\dot{\eta}$ flow is adequate to keep $n_2(z = o) \cong n_2(z = z_m)$. Then the value of $\dot{\xi}_2$ at any value of z is given by:

$$n_1 m_i \dot{\xi}_1^2 \left(1 - \frac{r_{co}^2}{r_c^2}\right) = \eta_2 m_i \dot{\xi}_2(z)$$

where $n_2 = \frac{9}{8} n_1$

so $$\dot{\xi}_2(z) = \dot{\xi}_1 \left(\frac{8}{9}\left(1 - \frac{r_{co}^2}{r_c}\right)\right)^{\frac{1}{2}}. \qquad (13)$$

An alternative calculation for $\dot{\xi}_2(z)$ is to assume that before any $\dot{\eta}$ velocity develops the mass flow equation which is applicable is $n_1 m_i \dot{\xi}_1 = n_2 m_i \dot{\xi}_2$. This equation, together with (2), (7) and (12), gives

$$\dot{\xi}_2(z) = \dot{\xi}_1 \left(1 - \frac{r_{co}^2}{r_c^2}\right). \qquad (14)$$

13. The velocity differential in the ξ direction in the shocked plasma between $z = o$ and $z = z_m$ is approximately $\dot{\xi}_2(z_m)$. This velocity differential which is a measure of the shear in velocity grows with time as

$$\dot{\xi}_2(z_m) = \frac{8}{9} \dot{\xi}_1 = \frac{8}{9} \frac{B_o \sin \omega t}{\sqrt{z \mu_o n_1 m_i}} \cong \frac{8}{9} \frac{B_o \omega t}{\sqrt{z \mu_o n_1 m_i}} \qquad (15)$$

for $\sin \omega t \cong \omega t$ and $\frac{r_{co}}{r_{cm}} = \frac{1}{3}$, if equation (7) is used.

14. The growth of B_θ can be computed roughly on a lumped-constant basis by assigning an inductance, $L \cong \frac{1}{3} \frac{\mu_o \delta z_m}{2\pi \cdot 1.5 r_c \cos \alpha}$ to the current loop on the periphery of the current sheet. The net emf driving current in the loop shown in Figs.1 and 2 is $E_\xi(z = o) - E_\xi(z = z_m)$.

Now $$E_\xi(z = o) = \frac{B_o^2 \sin^2 \omega t}{2\mu_o \cdot 2 n_1 \delta e}$$

For $z = z_m$, $$E_\xi(z_m) = \frac{B_o^2 \sin^2 \omega t}{2\mu_o \cdot 2 n_1 \delta e} \cdot \frac{1}{9} \frac{\dot{\xi}_1 + \dot{\xi}_2}{2\dot{\xi}_1} = \frac{B_o^2 \sin^2 \omega t}{4 \mu_o n_1 \delta e} \cdot \frac{1}{9}$$

Hence $$E_\xi(z = o) - E_\xi(z = z_m) \cong E_\xi(z = o) \qquad (16)$$

15. If we assign a resistance to the loop R, the differential equation for the lumped poloidal current i_p is

$$L \frac{di_p}{dt} + i_p R = \frac{B_o^2 \sin^2 \omega t}{4 \mu_o n_1 \delta e} \qquad (17)$$

In the early stages when the current is limited by L and $\sin \omega t \cong \omega t$,

$$i_p = \frac{1}{12} \frac{B_o^2 \omega^2 t^3}{\mu_o n_1 \delta e L}, \qquad (18)$$

and $B_\theta = \frac{\mu_o i_p}{2\pi \cdot 1.5 r_{co}}$. The B_θ which, in the early stages, grows as t^3 while the velocity shear in $\dot{\xi}_2$ grows only as t is of the <u>correct sign</u> to close this velocity shear into an eddy, just as it should also close the velocity shear into an eddy in the coaxial accelerator[3] when the center conductor is

negative. When the i_p is limited by the resistance R, the current,

$$i_p = \frac{B_o^2 \sin^2 \omega t}{4\mu_o n_1 \delta e R}$$

still grows more rapidly than the velocity shear which grows only as t or sin ωt. In this simple-shock model, the division of energy into translational and rotational energy can be estimated in the same way as was done for the coaxial plasma accelerator[3].

16. It is well to examine in more detail the process of closing the shear in the velocity $\dot{\xi}_2$ in the shocked plasma into an eddy which gives the $v_p \cong v_{poloidal}$ of the toroidal plasmoid which is ejected. Fig.3 shows schematically two different possibilities in the collision of two columns of plasma in the frame of reference of the shocked plasma in the vicinity of $z = \frac{z_m}{2}$. In Fig.3(a) the two columns with the shear in velocity $\dot{\xi}_2$ just touch each other at the center line $\eta = \frac{\eta_m}{2}$, and although the fields $E_\eta = \dot{\xi}_2 \times B_\theta$ exist as shown, no Lorentz currents or Hall currents flow. There is then no alternative of the velocities $\dot{\xi}_2$ in the columns.

17. Fig.3(b), on the other hand, describes the situation which actually exists in the conical θ pinch where a velocity η is picked up, as shown, within the shock. As time transpires the column ($\eta < \frac{\eta_m}{2}$) moves up into the column ($\eta > \frac{\eta_m}{2}$) as shown in Fig.3(c). The electric fields E_η can now drive braking currents, and the mutual deceleration of the two columns gives rise to the Hall electric fields $E_{H\xi}$. The resultant current $\mathbb{J}$ driven by both E_η and $E_{H\xi}$ produces the forces $\mathbb{J} \times \mathbb{B}_\theta$ on each column as depicted. These forces lead to the closing of the velocity shear $\dot{\xi}_2$ into an eddy as indicated. If B_θ were in the opposite direction, the $\mathbb{J} \times \mathbb{B}_\theta$ forces would oppose the closing of the eddy.

18. We must now investigate the effects of the poloidal Hall currents $\mathbb{J}_p \sim i_p$ produced by the differential in E_ξ along the co-ordinate η. Where the poloidal currents flow across B_a, there will be the force density $\mathbb{J}_p \times \mathbb{B}_a = \mathbb{f}_\theta$ shown in Fig.1, which is primarily on the electrons and produces the currents $\mathbb{J}_{\theta H}$ as shown. The way in which $\mathbb{f}_\theta = \mathbb{J}_p \times \mathbb{B}_a$ produces the θ currents is different from the way in which $E_{\theta\ ind}$ produces the induced θ currents, $\mathbb{J}_{\theta\ ind}$ because the former produces an angular momentum about the coil axis in the $\mathbb{f}_\theta$ direction and the latter produces no net angular momentum. The impulse density $\int_o^t \mathbb{f}_\theta dt = (r\dot{\theta})_e\, m_e \eta$ is imparted directly primarily to the electrons and they by collision can eventually impart this momentum to the positive ions, as $(r\dot{\theta}_i) m_i \eta$. It can be noted that in the region $z < \frac{z_m}{2}$ the current $\mathbb{J}_{\theta H}$ opposes the induced current $\mathbb{J}_{\theta\ ind}$ but that in the region $z > \frac{z_m}{2}$, $\mathbb{J}_{\theta H}$ adds to $\mathbb{J}_{\theta\ ind}$.

Thus the currents $\mathbb{J}_{\theta H}$ in some measure compensate for the shear in $\frac{B_2^2}{2\mu_o}$ which exists along η since they produce the perturbation poloidal magnetic field B_{pp} (shown in Fig.1). The B_{pp} in the $-\xi$ direction should be looked for experimentally in the region of $z \simeq \frac{z_m}{2}$. The θ angular momentum produced by $\mathbb{J}_\theta$ is in one direction for $z < \frac{z_m}{2}$ and in the other direction for $z > \frac{z_m}{2}$ as shown in Fig.1, and the vector sum of these two θ angular momenta should be zero. Therefore a net θ angular momentum (spin) in the toroidal plasmoid can exist only if some process separates one of these regions from the other. This separation is to be expected because it should be initiated by the magnetic pressure (arising from B_{pp} in the $-\xi$ direction) in the vicinity of $z = \frac{z_m}{2}$ (see Fig.1). Another way of visualizing the repelling force between the two regions $z < \frac{z_m}{2}$ and $z > \frac{z_m}{2}$ is that the currents, $_{\theta H}$, in the two regions are in opposite directions and therefore repel each other, as two oppositely directed ring currents should. Once the separation starts, the axial pinching action of the currents $\mathbb{J}_{\theta\ ind}$ should gather the plasma from the region $z < \frac{z_m}{2}$ into a ring current, which has a rotational angular momentum in the direction in which a positive ion would execute its gyrorotation in the field B_a. The plasma in the region $z > \frac{z_m}{2}$ is expected to be gathered together axially, again by the action of $\mathbb{J}_{\theta\ ind}$ (i.e. $B_{poloidal}$), and the resulting torus here should have an equal and opposite θ angular momentum. This latter torus, which is very likely the type which has been observed[1,2], should therefore be expected to have also a v_θ. This v_θ will not be observable on the surface of the torus because the torus is expected to be a force-free type structure whose circulationvelocity v should be anti-parallel with the resultant B throughout. Therefore the velocity v_θ should be observable only in the region near the circular center-line of the torus, i.e., v_θ is expected to be buried below the surface.

19. The experimental progress coupled with the foregoing analysis not only provides a reasonable hypothesis as to the origin of B_θ and $v_{poloidal}$, it also thus sheds an explanatory light on the origin of rotation in the θ pinch. We can now predict that a θ pinch with a cylindrical coil will, on a compression cycle, give rise to a triplet of vortex rings. The necessary shear in $\frac{B_a^2}{2\mu_o}$ and hence in E_ξ and $\dot{\xi}_2$ is provided by the flaring of B_a at each end of the cylindrical coil. If the magnetic field B_a is in the same sense as that shown in Fig.1, the vortex ring (ring 1) emitted at the right end of the cylindrical coil should be right-handed in both its $B_\theta + B_{poloidal}$ and its $v_\theta + v_{poloidal}$. The vortex ring (ring 2) emitted at the left end of the coil has B_θ in the opposite direction but v_θ in the same direction and should be left-handed in both $B_\theta + B_{poloidal}$ and $v_\theta + v_{poloidal}$. The third vortex ring (ring 3) should be collected by axial contraction into the midplane of the

cylindrical coil. Ring 3 has an angular momentum which is equal to the sum of the other two rings, which is just twice that of each of the other two. That is, if ring 3 has a spin of 1, then ring 1 and ring 2 each have a spin of $-\frac{1}{2}$. The rings 1 and 2 not only have the right-handedness and left-handedness which comes from $B_\theta + B_{poloidal}$ and $v_\theta + v_{poloidal}$; they also have the right-handedness and left-handedness in the same sense as that possessed by the anti-neutrino and the neutrino: the spin (v_θ) and the direction of translation are tied together.

20. Ring 3, before it is axially contracted, has B_θ and $v_{poloidal}$ of one sign on one side of the median plane and B_θ and $v_{poloidal}$ of the opposite sign on the other side of the median plane. These are expected to cancel one another during the axial contraction, leaving only v_θ and $B_{poloidal}$ for ring 3. Ring 3, once it has contracted, should contain no right-handedness or left-handedness of any kind. Rings 1 and 2 have relatively large diameters and large moments of inertia, and they are encountering a large radial component of B_a. Therefore, even though their magnetic moments are anti-parallel to the applied field B_a, it is unlikely that they will flip rapidly, if at all. However, ring 3, when it has been axially contracted, can be expected to start to flip, as observed by Clark and Wuerker[6] and by Bodin, Niblett, Green, et al[7]. If the effective ring current in ring 3 is i_3, and its radius is r_3, its magnetic moment is $\mu_3 = i_3 \pi r_3^2$. The torque $\mu_3 \times B_a$ which tends to produce the flipping must contend with the angular momentum, $I_3\omega_3$, of ring 3 and thus should produce a precessional angular frequency ω_3'. There is apparently some dissipative process which permits the angle γ between μ_3 and B_a to change from its inital value of 180° towards 90° and eventually toward 0. The aspect of the ring 3 as it is observed along the axis then should grow from a circle to an ellipse of increasing ellipticity. The major axis of this ellipse should be observed to rotate with the precessional frequency given by $|\mu_3 \times B_a| = I_3\omega\omega_3' = \mu_3 B_a \sin\gamma$. The excellent framing camera pictures by Niblett et al seem to show such an ellipse with increasing ellipticity and increasing observed speed of precession during the early stages. The above analysis should be amenable to quantitative verification through the observations by Niblett et al; the observations should make it possible to measure ω_3' and the ellipticity simultaneously as a function of time. The major axis of the observed ellipse should be initially $2r_3$. If the minor axis is called $2r_3'$, then $\frac{r_3'}{r_3} = \cos\gamma$, and we expect from the analysis that $\omega_3' = \frac{\mu_3 B_a \sin\gamma}{I_3\omega_3}$. Thus $\omega_3' \frac{r_3}{r_3'}$ should be proportional to $\tan\gamma$. It is to be expected that the ring will distort and disintegrate as γ approaches 90°.

21. A magnetic coupling loop located on the surface of the vacuum tube should be able to measure the radial component of μ_3 at the frequency ω_3'.

22. A cylindrical coil or two conical θ-pinch coils back-to-back should thus, as we have seen, produce a torus right-handed in B_θ and B_p at one end and another torus left-handed in B_θ and B_p at the other end on the first compression half-cycle. On the expansion portion of the first half-cycle the values of B_θ will reverse, but B_p remains the same, and another pair of toruses of opposite handedness should be produced if nothing interferes. On the second half cycle, on compression the B_θ's remain the same as on the compression in the first half cycle, but the B_p's are reversed, thereby reversing the handedness from the first half cycle compression, if nothing interferes, and so on.

23. The plasma vortex rings observed[1,2] to be produced in the conical θ pinch have v_p, B_θ and B_p in the directions which agree with the foregoing analysis.

24. The tendency towards the production of B_θ, $v_{poloidal}$, and v_θ should occur in all compression mirror machines and cusp machines as it does in the conical θ pinch. This tendency should also occur when plasma from a plasma gun is fired into a cusp or conical coil. This automatic formation of B_θ produces a certain amount of shear in the magnetic field and thus should offer some protection against flute instability. The assessment of this effect has not yet, to the authors' knowledge, been taken into account in the stability theories in mirror and cusp machines.

25. The parallelism between the asymmetry in the behaviour of the coaxial accelerator and the non-conservation of parity in weak interactions has already been noted[3,8]. This asymmetry in the coaxial accelerator should change its sign with charge conjugation C, i.e. with the substitution of anti-matter plasma for ordinary matter plasma. In the conical θ pinch, as in the production of plasmoids with a plasma gun[8], the left-handedness in a plasmoid with ordinary matter should turn to right-handedness if anti-matter plasma is used. The individual plasmoid structures are not invariant to space inversion, P, (equivalent to a mirror reflection) which changes right-handedness to left-handedness. They are not invariant to charge conjugation C, but are invariant to CP. They are invariant to time inversion. Time inversion reverses the sign of the resultant velocity in the helical velocity pattern, $v_\theta + v_{poloidal}$, and therefore does not reverse the handedness of $v_\theta + v_{poloidal}$. Time inversion reverses both the sign of translational velocity and v_θ(spin) and therefore does not reverse the handedness of the combination of these two. Time inversion does not reverse the handedness of $B_\theta + B_{poloidal}$. Thus, the parallelism between the production of right-handedness and/or left-handedness in plasmoids and the two-component neutrino theory of Lee and Yang[9,10] and non-conservation of parity is remarkable. However, there is no actual violation of parity conservation in either the cylindrical θ pinch or the conical θ pinch.

26. The experimental results and foregoing analysis on the production of right-handedness and/or left-handedness in plasmoids teaches us that right-handedness and left-handedness are a consequence of the fundamental property of nature that negative electricity (electrons) are light and positive electricity (protons) are heavy. The switch from matter to anti-matter reverses these electrical roles and, as we have already seen, changes right-handedness to left-handedness and vice versa, in all three forms: $B_\theta + B_{poloidal}$, $v_\theta + v_{poloidal}$ and $v_\theta + v_{translational}$. An interesting corollary to this lesson is that not only the right-handedness and the left-handedness would vanish if the plasma were made of positronium, but the plasmoids themselves would vanish. Indeed the spin or angular momentum in plasma structures in general is produced mainly through the action of Hall currents which depend upon the heaviness of protons and the lightness of electrons. The spin we speak of here is, of course, the spin which naturally develops out of velocity shear in a magnetic field, not that coming from a homo-polar device constructed by man. Likewise the right-handed or left-handed structures are those where the plasma develops its own, B_θ or B_z and not those created in a pinch with a B_z field from a coil such as Levine[11] produced in the U.S. and Golovin[12] produced in Russia.

27. Nesterikhin[13] has reported that his 'fountain pinch' produces cells of plasma, each containing its own B_θ and $B_{poloidal}$. These cells seem to evolve from a great turbulence which involves m = 1 (kink) instabilities. In the light of the foregoing analysis perhaps we can eventually understand how the shear in acceleration and hence in electric field which occurs in the kink of a pinch can drive θ Hall currents and create a B_z just as in the conical θ pinch the shear in acceleration drives poloidal Hall currents to create a B_θ.

28. The senior author (W.H. Bostick) wishes to express his thanks to S.Lafleur, C.Lafleur and F. Engelmann at Fontenay-aux-Roses with whom he had many clarifying discussions on this subject. The senior author also wishes to thank the National Science Foundation for the opportunities provided by its fellowship programme and EURATOM-CEA at Fontenay-aux-Roses and the U.K.A.E.A., Culham Laboratory where his work was performed.

REFERENCES

(1) Wells, D.R. Plasma rotation in a θ-pinch accelerator. Bull. Amer. Phys. Soc., series 2, vol.7, no.4, p.292, April, 1962.

(2) Wells, D.R. Observation of plasma vortex rings. Physics of Fluids, vol.5, no.8, pp.1016-1018, August, 1962.

(3) Bostick, W.H., and Nankivell, J. The role of Hall currents and plasma vortices in the planar current sheet in a coaxial plasma accelerator. CLM-R 21, September, 1962.

(4) Burkhardt, L.C. and Lovberg, R.H. Current sheet in a coaxial plasma gun. Physics of Fluids, vol.5, no.3, pp.341-347, March, 1962.

(5) Keck, J.C. Current distribution in a magnetic annular shock tube. Physics of Fluids, vol.5, no.5, pp.630-632, May, 1962.

(6) Clark, G.L. and Wuerker, R.F. Plasmoid rotation in a theta pinch. Space Technology Laboratories Inc., Report no.9844-0031-RU-000.

(7) Niblett, G.B.F. and Green, T.S. Culham Laboratory. (Private communication.)

(8) Bostick, W.H. On the non-conservation of parity in the production of plasmoids. Euratom-CEA report no. EUR-CEA-FC-176, August, 1962.

(9) Lee, T.D. and Yang, C.N. Question of parity conservation in weak interactions. Physical Review, 2nd series, vol.104, no.1, pp.254-258, October 1, 1956.

(10) Lee, T.D. and Yang, C.N. Parity non-conservation and a two-component theory of the neutrino. Physical Review, 2nd series, vol.105, no.5, pp.1671-5, March 1, 1957.

(11) Levine, M.A. The H-centered pinch. (Paper given at an AEC sponsored meeting on controlled thermonuclear research in Princeton, 1955. Levine's was the first work of this type in the U.S.).

(12) Artsimovitch, L. and Golovin, I. (Early work on the pinch effect with an included magnetic field, B_z. First revealed at the Symposium on Electromagnetic Phenomena in Cosmical Physics, Stockholm, 1956).

(13) Nesterikhin. (Private communication.)

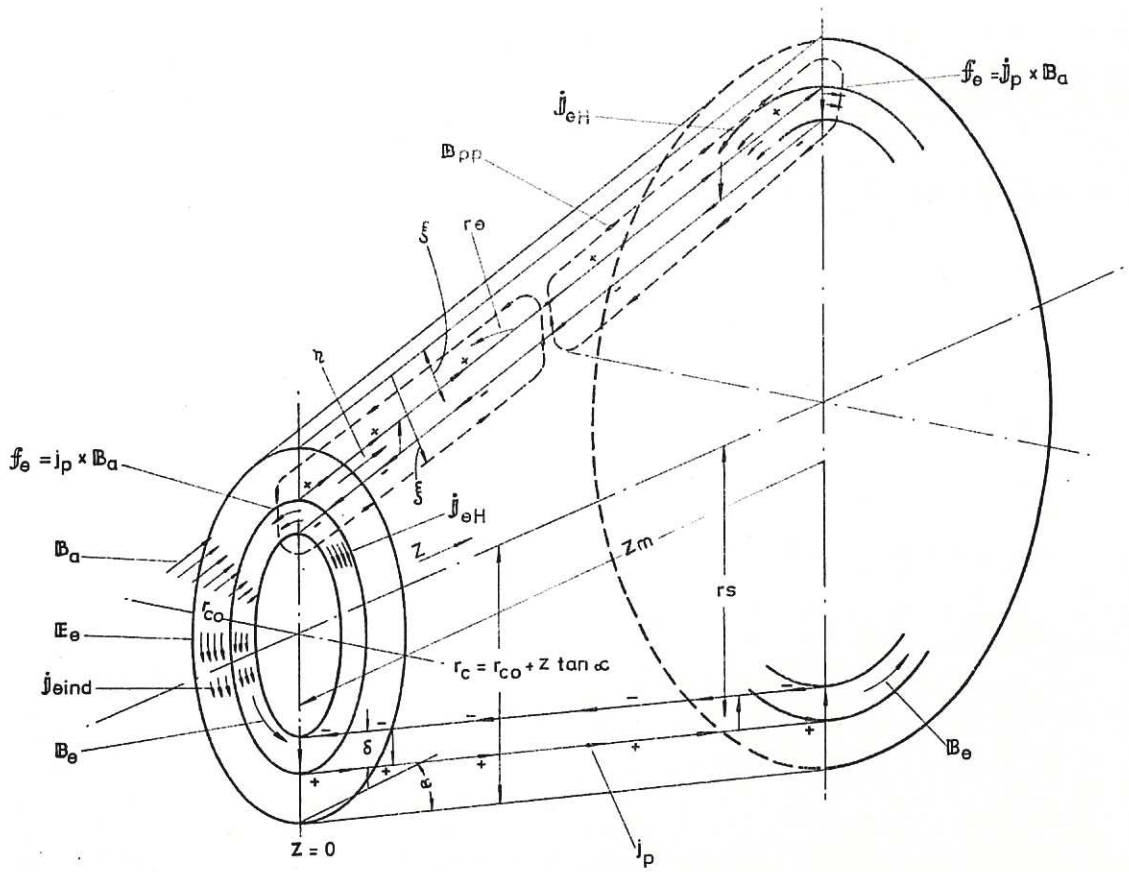

CLM - P 13 Fig. 1 Diagram of a conical θ pinch coil which generates a current sheet of thickness δ in the plasma by applying a magnetic field B_a.

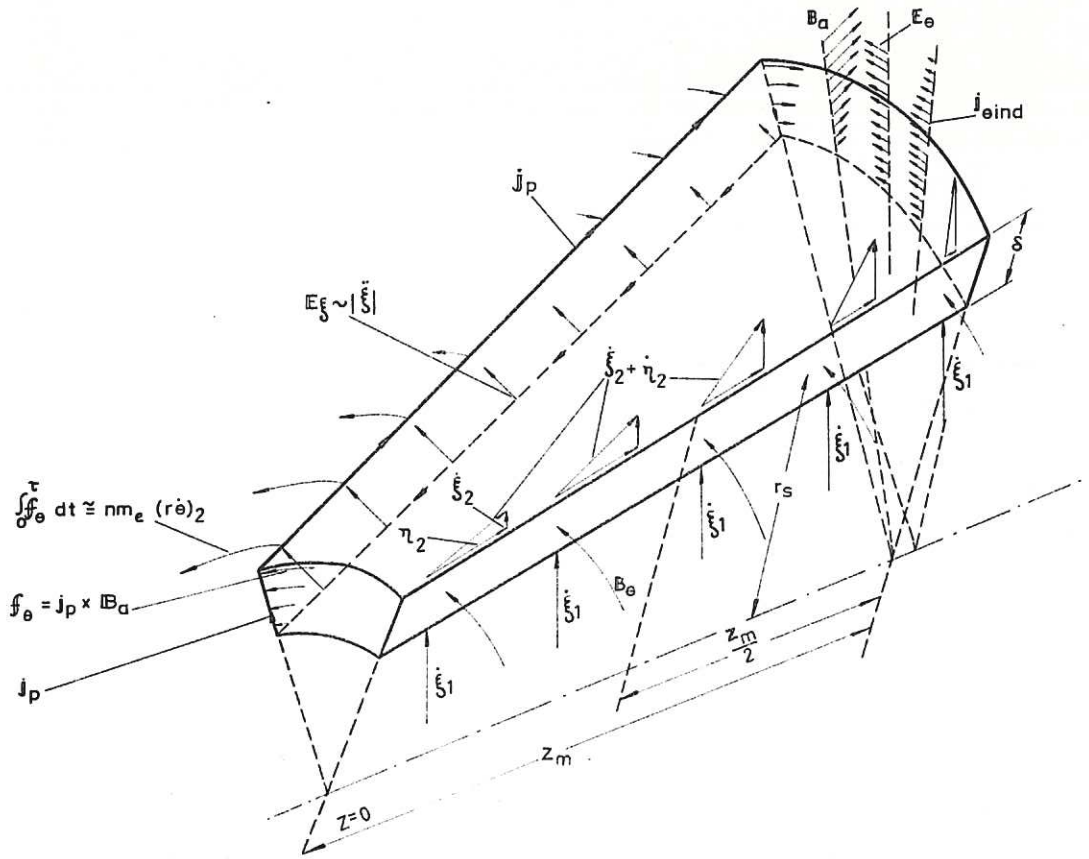

CLM - P 13 Fig. 2 Enlarged section of the current sheet. In the frame of reference of the current sheet the plasma approaches the sheet with a velocity $\dot{\xi}_1$, and recedes from the sheet with velocities which are the vector sum of $\dot{\xi}_1$ and $\dot{\eta}_2$ as shown.

CLM - P 13 Fig. 3 Schematic drawing of the effects which occur in the shocked plasma when a shear in $\dot{\xi}_2$ has been established in the presence of B_θ. The frame of reference is that for the plasma velocity at $z = \frac{z_m}{2}$

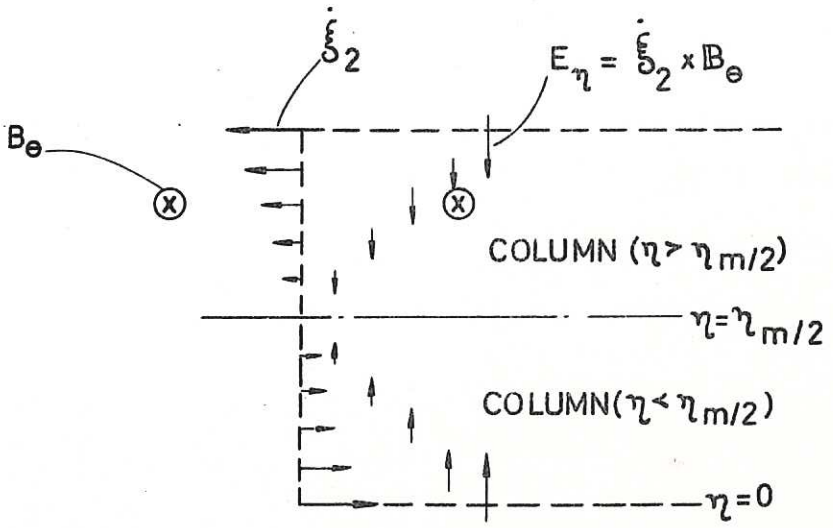

Fig. 3(a) An academic case where the two counter-streaming columns barely touch at $\eta = \frac{\eta_m}{2}$.

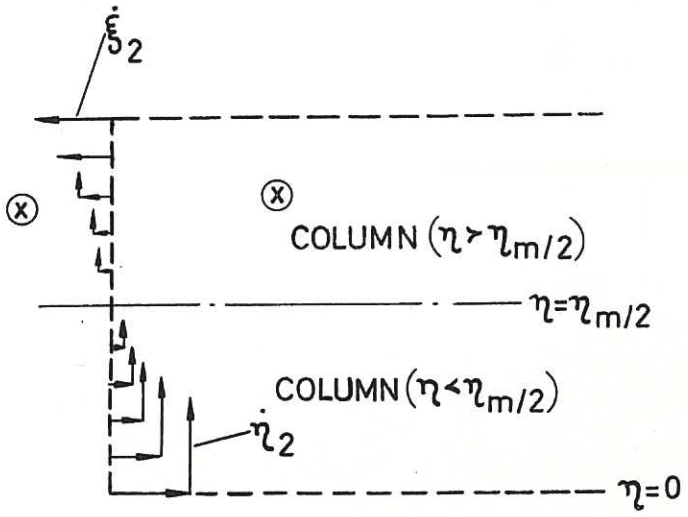

CLM - P 13 Fig. 3(b) The actual case in the conical θ pinch where the $\dot{\eta}$ produced within the sheet carries the lower column into the upper column.

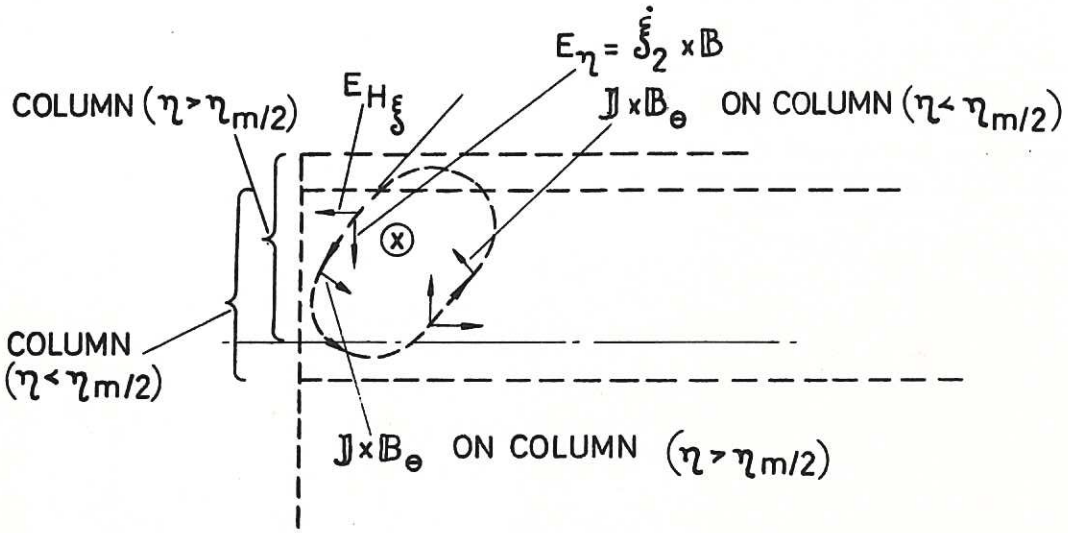

CLM - P 13 Fig. 3(c) The Hall currents and $\mathbb{J} \times \mathbb{B}_\theta$ forces which occur as the two columns stream through one another. The $\mathbb{J} \times \mathbb{B}_\theta$ forces are in the direction to close the velocity shear into an eddy.